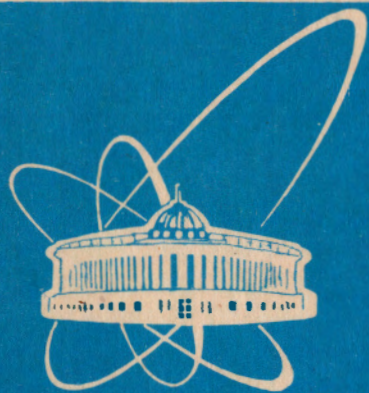


94-398



ОБЪЕДИНЕННЫЙ
ИНСТИТУТ
ЯДЕРНЫХ
ИССЛЕДОВАНИЙ
ДУБНА

E9-94-398

Hongwei Zhao*, A.A.Efremov, V.B.Kutner

CALCULATION OF GAS MIXING EFFECT
IN ECR ION SOURCE

Presented to the 7th International Conference on the Physics of Highly
Charged Ions, September, 1994, Vienna, Austria

*Permanent address: Institute of Modern Physics, Academia Sinica,
P.O.Box 31, 730000, Lanzhou, China

1 Introduction

The gas mixing effect has been widely used in many Electron Cyclotron Resonance (ECR) multicharged ion sources over the last few years because of its obvious advantage. The gas mixing effect consists in a substantial increase of the currents of high charge state ions when a second lighter gas, so-called support gas, is mixed into the plasma, meanwhile, the currents of low charge state ions are depressed by the gas mixing. The first observations of the beneficial effect of the gas mixing were reported by KVI and IKP-Julich groups[1]. Since then, the gas mixing has been rapidly applied in most of ECR sources. It is well known that the performances of ECR ion sources have been greatly improved by the use of the gas mixing, while there has been no satisfactory qualitative and quantitative explanation of its mechanism. Various explanations have been proposed in the past years by Geller[2], Antaya[3], and Delaunay[4]. They were reviewed by Drentje[1]. In previous explanations, they only used one single mechanism to explain the gas mixing effect, such as reduced average charge state[2], or ion cooling[3], and so on. Several attempts have been made to calculate the ion charge state distribution in the gas mixing situation. The pioneer work is due to Antaya[3] and Shirkov[5], and then followed by the others [6,7]. In previous calculation, they didn't consider the effect of thermal electrons, which is supposed to be very important in ECRIS plasma. Moreover, the previous ion confinement time was determined by the ambipolar diffusion of the ions and the ion mobility in the electric field established by the plasma potential, i.e. Jongen's model[8]. But the experiments have indicated that the plasma potential dip model for the ion confinement in ECRIS is more reasonable[9,10]. In order to understand the mechanism of the gas mixing effect, following the pioneer work of Antaya, Shirkov, Jongen, and West[11], we did a numerical calculation on the gas mixing effect. The basic code is due to West[11]. Particular emphases have been put on the effect of support gas upon the ion charge state distribution, the electron density, the average charge state, the plasma potential dip and the electron scattering rates.

2 Ion Confinement

We basically consider the ECR ion source as a mirror machine with hot electrons (a few keV), thermal electrons (a few tens eV), and cold ions (a few eV). Ion parallel confinement is dependent on the magnetic field configuration and potential. The effect of radial particle transport is neglected. The central plasma in an ECR ion source should dip because of a relatively high density and relatively long confinement time of hot electrons in the central region. So ions are electrostatically confined in the space-charge electric field of the hot electrons, i.e., confined by a small negative potential dip $\Delta\phi$, and most of them likely remain cold owing to the large ratio of the electron-ion energy equipartition time to the ion confinement time. We have assumed that all ion species are in thermal equilibrium at a same temperature. The ion confinement time is calculated by taking into account the ion diffusion time, the scattering time and the time for the ions to overcome the potential dip $\Delta\phi$, i.e. [11],

$$\tau_i = (\tau_f + \tau_s) \exp\left(\frac{\Delta\phi z_i}{T_{ion}}\right) \quad (1)$$

where $\tau_f = RL\left(\frac{\pi m_{ion}}{2T_{ion}}\right)^{\frac{1}{2}}$, $\tau_s = G(R)\tau_{si}\frac{\Delta\phi z_i}{T_{ion}}$
 τ_i is ion confinement time. R is mirror ratio. $G(R)$ is a factor, here approximately equal to 2. L is effective plasma length. T_{ion} is ion temperature. τ_{si} is the ion scattering time. z_i is ion charge state.

In view of the ion scattering time, we only consider the collisions between the ions since the mean free paths for the collisions of ion-electron and ion-neutral are much larger than that of ion-ion collisions, as large as five to seven orders of magnitude. We have

$$\tau_{si} = \frac{1}{\nu_{i\Sigma_j}} + \frac{1}{\nu_{i\Sigma_j'}} \quad (2)$$

where $\nu_{i\Sigma_j}$ is the collision rate of ion i with all the other ions of same species. $\nu_{i\Sigma_j'}$ is the collision rate of ion i with all the other ions of different species, i.e. collisions between the ions

of main gas and the ions of support gas. These collision rates were quoted from Ref.[11,12].

3 Hot Electrons and Thermal Electrons

Hot electrons are created by ECR heating and confined magnetically in the minimum-B geometry of ECRIS. They move back and forth along the magnetic field lines and when crossing the resonance zone, they receive kicks of transverse energy from the rf electric field that helps trap them in the B_z mirror magnetic field, and eventually reach higher energies[9]. The hot electrons might escape from the magnetic confinement and be lost, either because they hit on the wall of the plasma chamber, or because they diffuse into the loss-cone by a large angle scattering. The scattering time of hot electrons is much larger than the bounce period between the two mirror peaks. We suppose the hot electron lifetime is basically determined by large angle scattering with the other electrons, the ions and the neutrals in the plasma, here including the ions and the neutrals of support gas, i.e.,

$$\tau_e^h = \frac{1}{\nu_{ee}} + \frac{1}{\nu_{e\sum i}} + \frac{1}{\nu_{e\sum n}} \quad (3)$$

where τ_e^h is the lifetime of the hot electrons, ν_{ee} , $\nu_{e\sum i}$, $\nu_{e\sum n}$ are collision rates of electron-electron, electron-ion, and electron-neutral, which were got from Ref.[11,12].

Thermal electrons are produced mainly by the hot electron impact ionization. They are generally considered to be confined by a positive plasma potential. Collisions are very important for thermal electrons, and the effective lifetime for thermal electrons can be calculated by 90° Spitzer collisions and the plasma potential[11,12].

We assume that the hot electron density and the thermal electron density are uniformly distributed in the plasma. The quasineutrality for all ions and electrons throughout the plasma is required,

$$n_e^{th} = \sum_{i=1}^{imaxA} Z_i^A n_i^A + \sum_{i=1}^{imaxB} Z_i^B n_i^B - n_e^h \quad (4)$$

Where n_e^{th} and n_e^h are the densities of thermal electrons and hot electrons. Z_i^A and Z_i^B are the ion charge state of main gas and support gas. n_i^A and n_i^B are the ion densities of main gas and support gas with charge state i .

The thermal electron density in the confined plasma is related to the thermal electron density in the mirror throat by[11]

$$n_e^{th} = n_{em}^{th} \exp\left(\frac{\Delta\phi}{T_e^{th}}\right) \quad (5)$$

where n_{em}^{th} is the thermal electron density in the mirror throat. It is determined by the ionization rate and the ion flow time. T_e^{th} is the thermal electron temperature.

In present work, the hot electron density is an input parameter. The thermal electron density and the potential dip are calculated through a self-consistent between eq.(4) and eq.(5), which are realized by means of Newton-Raphson Method[11].

4 The neutrals in the plasma

In the plasma of an ECR source, there is a continuous burn up of neutrals through electron impact ionization, as well as through charge exchange with ions. There is also a continuous neutral flux entering and leaving the plasma. Due to the imperfect nature of the plasma confinement, ions escape from the plasma and get neutralization when they hit the wall. A large part of the neutrals generated at the wall are reionized by the plasma or are pumped by the system vacuum pumps. The distribution of the neutral density in the plasma of a real ECR ion source is quite inhomogenous. The neutral density outside the confined plasma, especially near the wall, is much higher than that inside the confined plasma. The neutral density from the wall to the plasma center might decrease exponentially. However, considering calculation simplicity, we assumed the neutrals inside and outside the plasma are kept in uniform distribution respectively. It is also assumed that

a dynamic equilibrium exists between the neutral density outside the plasma and the neutral density inside the plasma. We note that the mean free paths for neutral-ion collisions are large compared with the chamber dimensions, and for this reason we expect the neutrals to take on the temperature of the wall and not equilibrate with the much hotter ions. In the calculation of neutral density inside the plasma, we only consider single step ionization, single step charge exchange, and the neutral flux entering into and leaving out of the plasma. It should be underlined here that the charge exchange between the ions of main gas and the neutrals of support gas, the ions of support gas and the neutrals of main gas play an important role in determining the ion charge state distribution and the neutral density inside the plasma.

The change rate of neutral density inside the plasma for main gas A can be written as

$$\begin{aligned} \frac{dn_{npl}^A}{dt} = & \nu_0^A n_0^A + n_1^A \langle \sigma_{ix}^{AH} v_i^A \rangle_{1-0} n_{npl}^B - n_i^h \langle \sigma_i^A v_i^h \rangle_{0-1} n_{npl}^A - \\ & n_i^{th} \langle \sigma_i^A v_i^{th} \rangle_{0-1} n_{npl}^A - \sum_{i=2}^{imaxA} n_i^A \langle \sigma_{ix}^{AA} v_i^A \rangle n_{npl}^A - \\ & \sum_{i=2}^{imaxB} n_i^B \langle \sigma_{ix}^{BA} v_i^B \rangle n_{npl}^A - \nu_0^A n_{npl}^A \end{aligned} \quad (6)$$

Where ν_0^A is the rate of the neutral flux entering into (leaving out of) the plasma. n_0^A is the neutral density outside the plasma for main gas A . n_{npl}^A and n_{npl}^B are the neutral densities inside the plasma for main gas A and support gas B . σ_{ix}^{AH} , σ_{ix}^{AA} , σ_{ix}^{BA} are the charge exchange cross sections between the ions of main gas A and the neutrals of support gas B , the ions of main gas and the neutrals of main gas, the ions of support gas and the neutrals of main gas respectively. v_i^A and v_i^B are the thermal velocities for main ions and the ions of support gas. v_i^h and v_i^{th} are the thermal velocities for the hot electrons and the thermal electrons.

At an equilibrium of stationary state, $\frac{dn_{npl}^A}{dt} = 0$.

Interchanging the symbol A and B in eq.(6), we can get an equation of the neutral density inside the plasma for support gas B .

5 Balance Equations for the Ion Charge State Distribution

Positive ions in ECR ion source are produced mainly by successive electron impact ionization from neutral to maximum charge state. In Present model, all the multiple processes, such as multiple ionization and charge exchange, are negligible, although the importance of single-step multiple ionization processes and auto-ionizing metastable states, particularly for low and intermediate charge ions, is becoming more apparent[13]. The most important and effective contribution to the reduction of a given charge state is charge exchange between ions and neutrals. However, at the higher charge states, we have to take into account radiative recombination resulting from the thermal electrons. The importance of dielectronic recombination for reducing charge state has become recognized. Fortunately, this effect is usually small compared with charge exchange, and then neglected here. The ions and the neutrals of support gas take part in all the same processes as those of the main gas. The interaction between them is nothing more but elastic collisions and charge exchange. The balance equations for the ions of support gas and main gas are treated separately.

For the ions of main gas A with charge state i ($2 < i < imax - 1$), the equilibrium equation that we wish to solve is described by

$$\begin{aligned} \frac{dn_i^A}{dt} = & n_i^h \langle \sigma_i^A v_e^h \rangle_{i-1,i} n_{i-1}^A + n_i^{th} \langle \sigma_i^A v_e^{th} \rangle_{i-1,i} n_{i-1}^A + \\ & n_{i+1}^A \langle \sigma_{ex}^{AA} v_i^A \rangle_{i+1,i} n_{i+1}^A + n_{npl}^B \langle \sigma_{ex}^{AB} v_i^A \rangle_{i+1,i} n_{i+1}^A + \\ & R_{i+1,i}^A n_{i+1}^A + \frac{n_i^A}{L} n_i^{0A} - n_e^h \langle \sigma_i^A v_e^h \rangle_{i,i+1} n_i^A - \\ & n_i^{th} \langle \sigma_i^A v_e^{th} \rangle_{i,i+1} n_i^A - n_{npl}^A \langle \sigma_{ex}^{AA} v_i^A \rangle_{i,i-1} n_i^A - \\ & n_{npl}^B \langle \sigma_{ex}^{AB} v_i^A \rangle_{i,i-1} n_i^A - R_{i,i-1}^A n_i^A - \frac{n_i^A}{\tau_i^A} \end{aligned} \quad (7)$$

Where $R_{i+1,i}^A$ the rate of radiative recombination from charge state $i+1$ to i , which can be calculated from [11]. $\frac{n_i^A}{\tau_i^A}$ indicates the ion flux out of the plasma. $\frac{v_i^A}{L} n_i^{0A}$ the input ion flux from

the first stage. n_i^{0A} is the density of main ions from the first stage. The other symbols in Eq.(7) have the same meaning as those in Eq.(6).

The eq.(7) is only strictly valid for the ions $2 < i < imax - 2$.

The single charged ions in ECR ion source are involved in a different processes. The resulting equation for the single charged ions of the main gas A is given by

$$\begin{aligned}
 \frac{dn_1^A}{dt} = & n_i^h \langle \sigma_i^A v_i^h \rangle_{>0,1} n_{npl}^A + n_i^{th} \langle \sigma_i^A v_i^{th} \rangle_{>0,1} n_{npl}^A + \\
 & n_{npl}^A \langle \sigma_{rx}^{AA} v_i^A \rangle_{>2,1} n_2^A + n_{npl}^B \langle \sigma_{rx}^{AB} v_i^A \rangle_{>2,1} n_2^A + \\
 & \sum_{i=2}^{imaxA} n_i^A \langle \sigma_{rx}^{AA} v_i^A \rangle_{>i,i-1} n_{npl}^A + \sum_{i=2}^{imaxB} n_i^B \langle \sigma_{rx}^{BA} v_i^B \rangle_{>i,i-1} n_{npl}^A + \\
 & \frac{v_i^A}{L} n_1^{0A} - \frac{n_1^A}{\tau_1^A} - n_i^h \langle \sigma_i^A v_i^h \rangle_{>1,2} n_1^A - \\
 & n_i^{th} \langle \sigma_i^A v_i^{th} \rangle_{>1,2} n_1^A - n_{npl}^B \langle \sigma_{rx}^{AB} v_i^A \rangle_{>1,0} n_1^A
 \end{aligned} \quad (8)$$

Radiative recombination is negligible for those low charge state.

At equilibrium, $\frac{dn_1^A}{dt} = \frac{dn_1^A}{dt} = 0$.

For the ions of support gas, we only need interchange the symbol A and B .

Eq.(4),(6),(7) and (8) are the main equations in present work, which are solved as a set of nonlinear algebraic equations by an iterative numerical method. The iterative numerical procedure is dependent on the self-consistent determination of the thermal electron density and the plasma potential dip by means of Newton-Raphson method[11]. We take a Maxwell-Boltzman distribution for the electron energy, and Lotz formula[14] for the electron impact ionization cross section. The ionization potential and subshell binding energies are taken from Ref.[15]. The approximated formulas for charge exchange cross sections which involve the same and different species are used from Ref.[16].

6 Extraction Ion Current and Average Charge State

The extraction current of the main ions from an ECR ion source can be expressed as

$$I_{ex} = \eta e n_i^A Z_i^A L S / \tau_i^A \quad (9)$$

Where η is the percentage that the ions with charge state Z_i^A could be really extracted from the source. e is the electric charge. L is the effective plasma length. S is the extraction area. In order to make a reasonable comparison of ion currents got under different conditions (in fact, we also don't know how much η is), in our work we use an ion current normalized to a current of certain charge state (here A_r^{A+}) with no gas mixing. This normalized ion current is exactly proportional to the real current extracted from an ECR source.

The average charge state used in this work is expressed by

$$\langle q \rangle = \frac{n_r^h + n_r^{th}}{\sum_{i=1}^{imaxA} n_i^A + \sum_{i=1}^{imaxB} n_i^B} \quad (10)$$

7 Calculation Result

We present the main calculation results in the equilibrium state of Argon plasma mixed with Oxygen. The code was written such that it can be run with and without gas mixing. The code input parameters are neutral densities of main gas A , and support gas O_2 outside the plasma (n_0^A, n_0^B), hot electron density n_e^h and temperature T_e^h , thermal electron temperature T_e^{th} , ion temperature T_i , mirror ratio R , source dimensions, and atomic physics data for main gas and support gas. The typical range of input parameters is from the operation experiences of present ECR ion sources: $n_e^h = 10^{11} \sim 1.5 \times 10^{12} \text{cm}^{-3}$, $T_e^h = 1 \sim 20 \text{keV}$, $T_i = 3 \sim 20 \text{eV}$, $T_e^{th} = 20 \sim 100 \text{eV}$, $n_0^A + n_0^B = 10^9 \sim 10^{11} \text{cm}^{-3}$, $R = 2$, mirror to mirror length $L = 20 \sim 45 \text{cm}$, diameter of the plasma chamber $D = 7 \text{cm}$. The running of the code is quite dependent on a good match among those input plasma parameters, otherwise the code would fail to reach a self-consistent convergence

in the calculation of thermal electron density and the plasma potential dip. The iterative numerical procedure starts with an initial evaluation of the charge state distributions (CSD) for the ions of the main gas and the support gas, and then calculates the ion confinement time and the neutral densities inside the plasma. Finally the new CSD are calculated. If the criterion for convergence is not satisfied, the code enters the next iteration.

First, keeping the total neutral density ($n_0^A + n_0^B$) outside the plasma and the other parameters constant, we only change the mixture ratio between the neutral densities of the main gas and the support gas outside the plasma. Fig.1 shows the charge state distributions with different mixture ratio between main gas A , and support gas O_2 . We can see from Fig.1 that support gas O_2 does shift the CSD to the higher charge state, meanwhile, the currents of lower charge state are depressed. With increasing the support gas O_2 percentage (decreasing the main gas A , percentage), this effect is more obvious. But when support gas O_2 is dominant up to 98%, only very high charge states benefit from the presence of the support gas O_2 . When the ion currents are normalized to the total currents, the charge state distributions in this case (same as Fig.1) are demonstrated in Fig.2 . Fig.2 means nothing but the percentage of certain ion charge state in the total currents. The ion confinement time corresponding to Fig.1 is shown in Fig.3. It seems that the ion confinement time is very sensitive to the mixture ratio between the main gas and the support gas. That is because the multicharged ions are confined by a small negative potential dip $\Delta\phi$ which is sensitive to the gas pressure and the mixture ratio. Our calculation indicates that the potential dip increases with increase of the support gas percentage, as shown in Fig.4. The plasma potential, the electron scattering rate, and the average charge state decrease with increase of the support gas percentage, as shown in Fig.5,6,7.

Making the neutral density of the main gas A , constant, and varying the neutral density of the support gas O_2 step by step, we find that the thermal electron density keeps rising with increase of the support gas density, as shown in Fig.8. The dependence of the electron scattering rate on the support gas

density in this case is illustrated in Fig.9. The increase of the support gas density brings down the electron scattering rate, But when the density of the support gas is raised up to certain value, the collisions between electrons and neutrals might be dominant, and hence the electron scattering rate rises rapidly. It is obvious that the average charge state decreases with increase of the support gas density (Fig.10). As an example, the dependences of $A_{7,12+}$ currents upon the support gas density and the main gas density are indicated in Fig.11 and Fig.12 respectively. The varying tendency is consistent with that of experimental results.

The effect of ion temperature on the charge state distribution is also studied numerically, as shown in Fig.13. The lower ion temperature is really beneficial to the higher charge states. As previous calculations, the ion charge state distribution is very sensitive to the density and temperature of the hot electrons, as shown in Fig.14, 15.

In order to check our calculation results, we make a comparison with the experimental results from Grenoble CAPRICE source [17] and LBL AECRIS [18], as shown in Fig.16,17. We can see the calculation CSD and the experimental results are in a good agreement. Of course, such comparison is very rough, which can only be regarded as a test to the code.

8 Conclusion and Discussion

There are so many parameters involved in the ECRIS plasma. They are related and interacted one another. When the light support gas is mixed into the ECRIS plasma, by ion-ion collisions, part of energy will be transformed from the ions of main gas to the ions of support gas. The reduction of kinetic energy of the main ions results in a better confinement. Meanwhile, lower ion temperature causes an increase of ion-ion collision frequencies and a decrease of ion-neutral charge exchange rates. All of these are beneficial to the formation of more ions with high charge state. On the other hand, because of mixing large amounts of light support gas into the ECRIS plasma, the average charge state in the plasma will decrease and therefore the

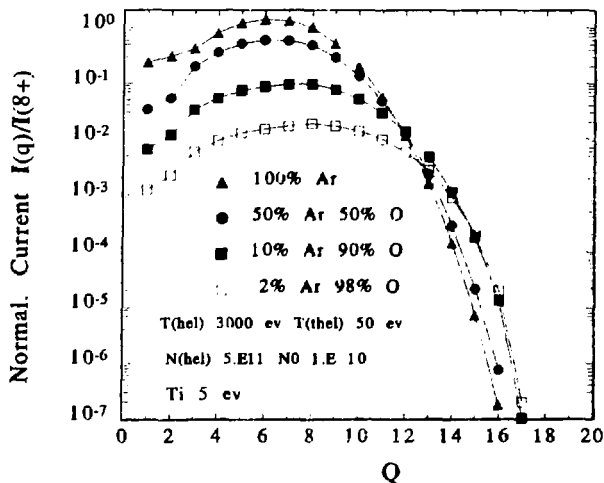


Fig.1. Charge state distribution for different ratio between the main gas and the support gas. All the ion currents are normalized to the current of Ar^{8+} without support gas.

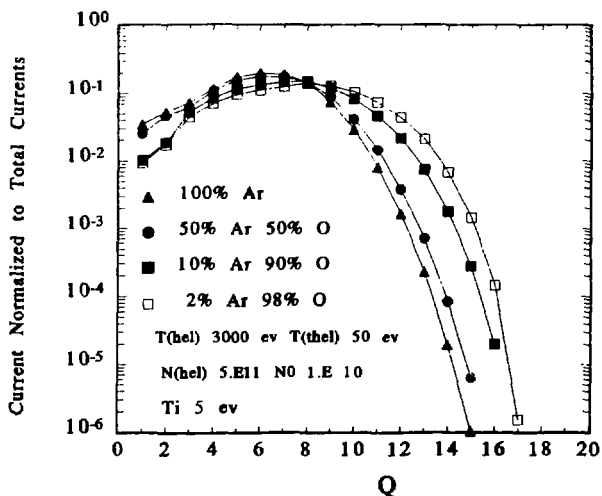


Fig.2. Same as Fig.1 except that the ion currents are normalized to the total currents of themselves.

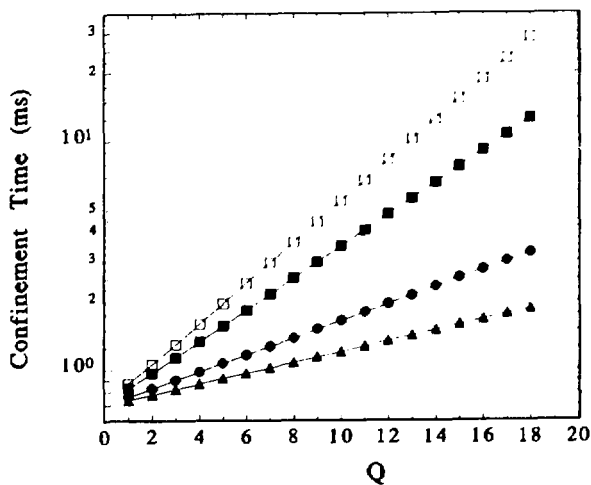


Fig.3. Ion confinement time versus different ratio between the main gas and the support gas (corresponding to Fig.1)

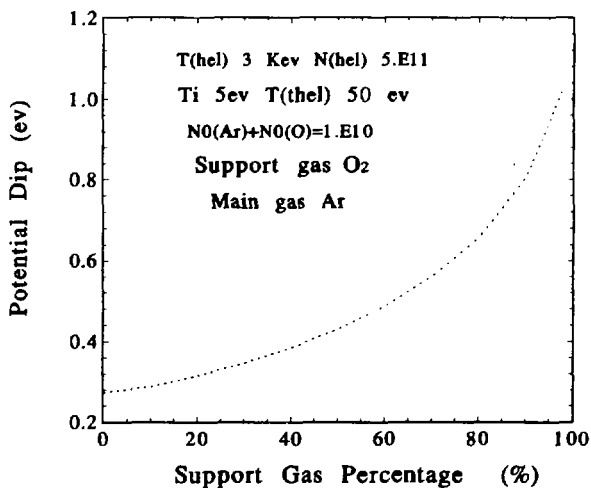


Fig.4. Dependence of the plasma potential dip on the support gas percentage, keeping the total gas density constant.

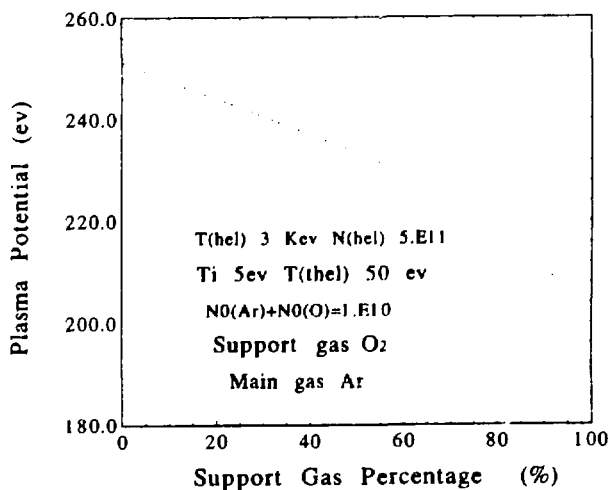


Fig.5. Dependence of the plasma potential on the support gas percentage, keeping the total gas density constant.

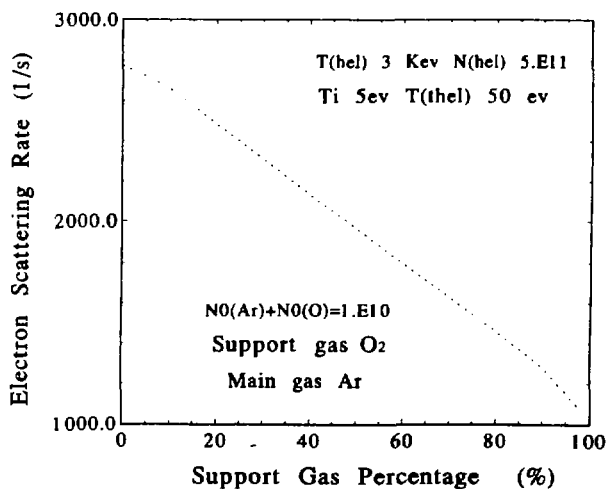


Fig.6. Dependence of the electron scattering rate on the support gas percentage, keeping the total gas density constant.

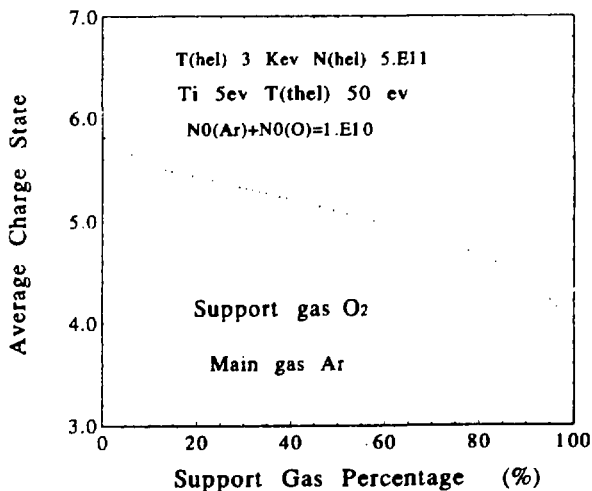


Fig.7. Dependence of the average charge state on the support gas percentage, keeping the total gas density constant.

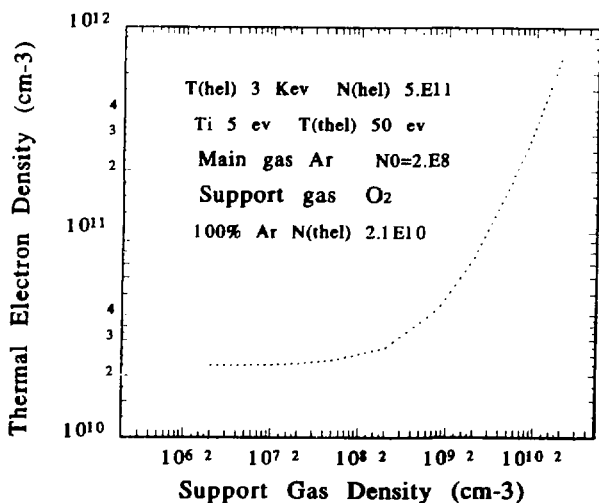


Fig.8. Dependence of the thermal electron density on the support gas density, keeping the main gas density constant.

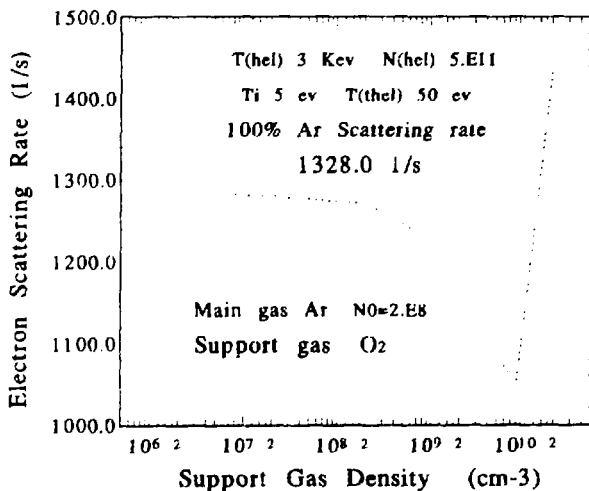


Fig.9. Dependence of the electron scattering rate on the support gas density, keeping the main gas density constant.

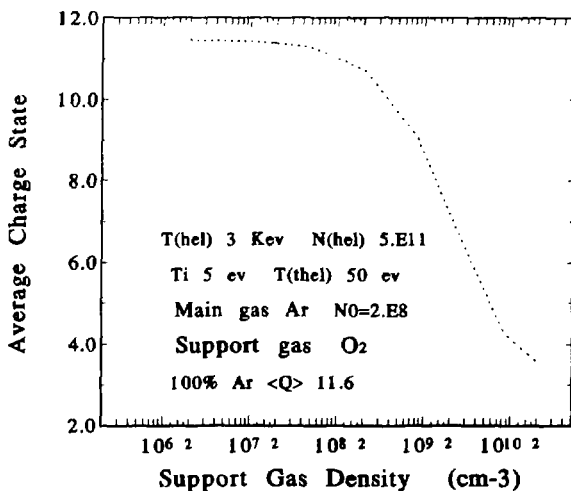


Fig.10. Dependence of the average charge state on the support gas density, keeping the main gas density constant.

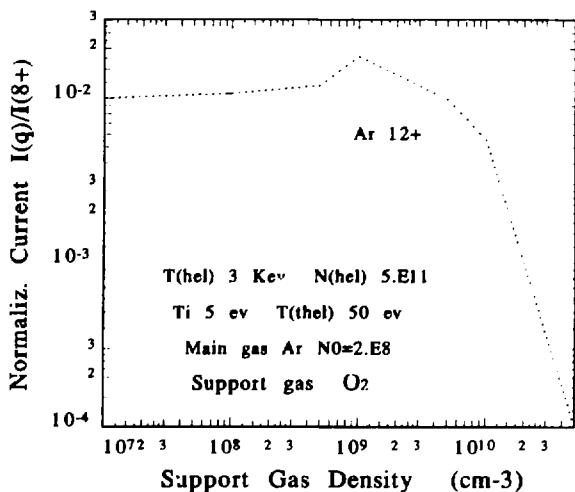


Fig.11. Normalized current of Ar^{12+} versus the support gas density, keeping the main gas density constant.

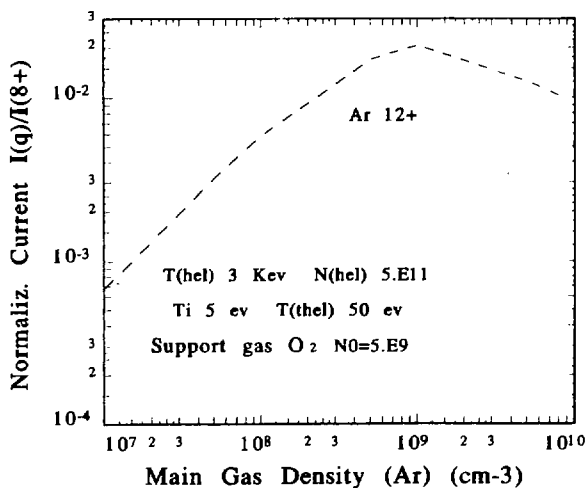


Fig.12. Normalized current of Ar^{12+} versus the main gas density, keeping the support gas density constant.

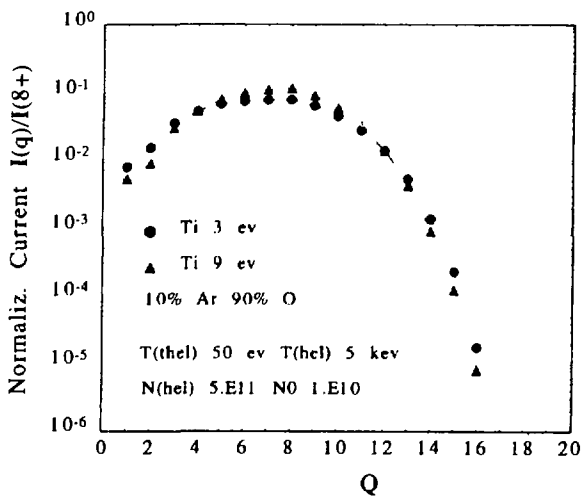


Fig.13. Charge state distribution for different ion temperature.

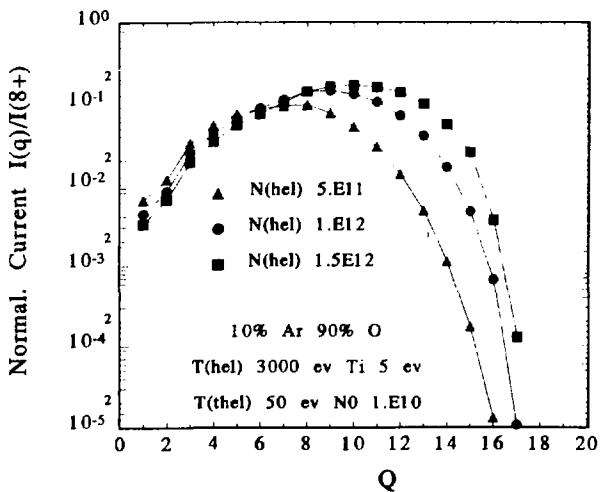


Fig.14. Charge state distribution for different hot electron density.

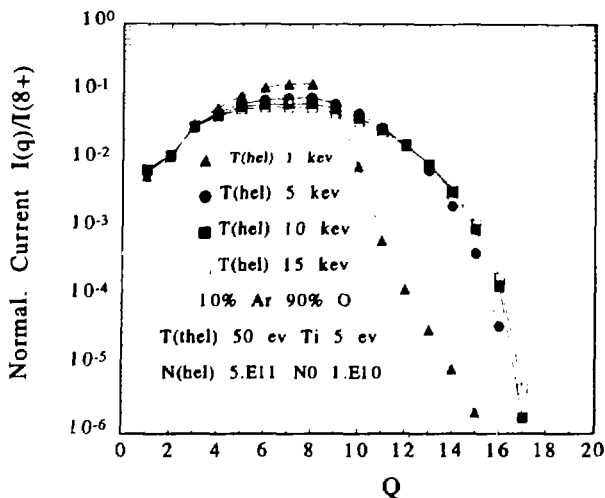


Fig.15. Charge state distribution for different hot electron temperature.

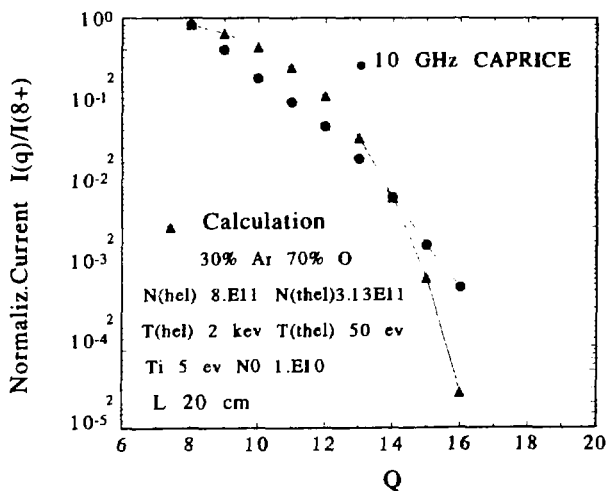


Fig.16. Comparison between the calculation and experimental results got from 10 GHz CAPRICE.

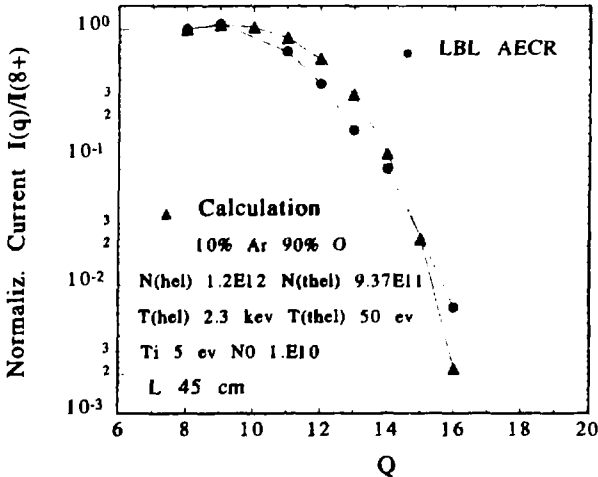


Fig.17. Comparison between the calculation and experimental results got from LBL AECRIS.

energy lifetime will increase allowing to reduce the RF power losses on the wall through ambipolar diffusion, which leads to a decrease of the turbulence level and improvement to ion confinement[2]. The lower average charge state sets a less electron scattering rates with ions and neutrals in the plasma, and thus improves the lifetime of the electrons. This brings about rise of the electron density and temperature, which results in higher ionization efficiency, decrease of the plasma potential and increase of the potential dip, hence an enhancement of ion confinement and more high charge state ions. In addition, the charge exchange processes between the ions of support gas and the neutrals of main gas give more ions with charge state 1 and 2, which increases the densities of high charge state ions by step-wise ionization.

It might be difficult to explain the gas mixing effect by only one single mechanism since it is involved in so many plasma parameters and they are related one another. Our preliminary calculations seem to indicate that it might be the combination of several factors that results in the gas mixing effect in ECR ion sources. Probably support gas causes these factors

simultaneously, such as ion cooling; increase of the electron density and the potential dip; decrease of the average charge state, the electron scattering rate and the plasma potential; and the charge exchange between the ions of support gas and the neutrals of main gas. Anyway, the further investigations are necessary before the mechanism can be clarified.

REFERENCE

- [1]. A.G.Drentje, Proceedings of the 11th International workshop on ECRIS, Groningen, 155, 1993.
- [2]. R.Geller, Proceedings of 8th workshop on ECRIS, East-lansing, NSCL, Rep. MSUCP-47, 1, 1987.
- [3]. T.Antaya, J. De. Phys. C1, 707, 1989.
- [4]. M.Delaunay, Rev.Sci.Instrum. Vol.63, 2861, 1992.
- [5]. G.Shirkov, Rev. Sci. Instrum. Vol.63, 2894, 1992.
- [6]. R.Baskaran, et al, Rev. Sci. Instrum. Vol.64, 191, 1993.
- [7]. J.Puerta, et al, Proceedings of the 11th International workshop on ECRIS, Groningen, 213, 1993.
- [8]. Y.Jongen, Proceedings of Workshop on ECR Ion Sources and Related Topics, Darmstadt, GSI81-1, 73, 1980.
- [9]. G.Melin, et al, Rev. Sci. Instrum. Vol.61, 236, 1990.
- [10]. J.Petty, et al, J. De. Phys. C1, 783, 1989.
- [11]. H.I.West, Lawrence Livermore National Laboratory, UCRL-53391, 1982.
- [12]. L.Spitzer, Physics of Fully Ionized Gases, 2nd ed. 1962.
- [13]. T.Antaya, Proceedings of the 11th International workshop on ECRIS, Groningen, 47, 1993.
- [14]. W.Lotz, Z. Physik Vol.220, 466, 1969.
- [15]. T.A.Carlson, et al, Atomic Data, Vol.2, 63, 1970.
- [16]. A.Muler, et al, Phys. Letters, 62A, 391, 1977.
- [17]. D.Hitz, et al, Proceedings of the 11th International workshop on ECRIS, Groningen, 91, 1993.
- [18]. C.M.Lyneis, et al, Proceedings of the 10th International Workshop on ECR Ion Sources, Knoxville, Tennessee, 47, 1990.

Received by Publishing Department
on October 14, 1994.